



International Conference on Structural Integrity 2023 (ICSI 2023)

# Evaluating hydrogen embrittlement susceptibility of a 2205 DSS

L.B. Peral<sup>a,b,\*</sup>, A. Díaz<sup>b</sup>, R. Rodríguez Aparicio<sup>b</sup>, J.M. Alegre<sup>b</sup>, I.I. Cuesta<sup>b</sup>

<sup>a</sup>University of Oviedo, C/Wifredo Ricart s/n, Gijón 33203, Spain

<sup>b</sup>University of Burgos, Avenida de Cantabria s/n, Burgos 09006, Spain

## Abstract

Hydrogen embrittlement of a 2205 DSS has been evaluated by in-situ tensile tests at high-pressure hydrogen gas. Mechanical tests were conducted in smooth and notched samples, following the ASTM G142 standard. Hydrogen embrittlement susceptibility was studied at 70 and 140 bar. In the smooth samples, the loss of ductility was marked. However, the increase in hydrogen pressure from 70 to 140 bar seems to be practically negligible. On the other hand, in the notched samples, hydrogen damage was especially remarkable at 140 bar. Finally, hydrogen embrittlement susceptibility is also discussed based on the fracture micromechanisms.

© 2023 The Authors. Published by Elsevier B.V.

This is an open access article under the CC BY-NC-ND license (<https://creativecommons.org/licenses/by-nc-nd/4.0>)

Peer-review under responsibility of the scientific committee of the ICSI 2023 organizers

*Keywords:* 2205 DSS, in-situ tensile tests, hydrogen embrittlement, fracture micromechanisms

## 1. Introduction

Energy transition in the European Union is expected to require hydrogen to represent a 24% of the EU total energy demand in 2050. One of the main challenges in the optimisation of hydrogen transport and storage lies in the selection of materials that can operate under high-pressure hydrogen in safe conditions while keeping a reasonable cost per stored H<sub>2</sub> kg. In this regard, the use of duplex stainless steels (DSS) represents a feasible alternative to control hydrogen susceptibility. For instance, in comparison to carbon or CrMo steels, DSS promise the optimized performance both in strength (because of the ferrite phase) and corrosion resistance (due to the austenite phase). The

\* Corresponding author.

E-mail address: [luisborja@uniovi.es](mailto:luisborja@uniovi.es)

balance between strength and hydrogen embrittlement susceptibility can be optimised by controlling the austenite/ferrite content and its microstructural features, such as grain size or band spacing. Nevertheless, hydrogen-induced degradation of DSS has attracted the attention of many researchers. V. Arniella et al. [1] studied the effect of hydrogen on 2205 duplex stainless steel using in-situ hydrogen electrochemical charging tensile tests. Hydrogen embrittlement susceptibility increased as current density increased because of the higher hydrogen activity provided by the aqueous electrolytic medium. Additionally, hydrogen damage also increased when the displacement rate decreased. L. Claeys et al. [2] also evaluated hydrogen-assisted cracking in 2205 duplex stainless steel by in-situ hydrogen charged tensile tested samples. Hydrogen embrittlement sensitivity increased with the electrochemical hydrogen charging time, with cracks propagation through austenite, ferrite and their interface. In addition, an additional challenging complication to the study of hydrogen-assisted cracking in DSS are the martensitic transformations taking place in austenite because of straining. More studies are still needed to understand the role of strain-induced martensite formation in hydrogen damage [2,3].

In our work, hydrogen embrittlement of a 2205 DSS (hot-rolled with solution annealed) was evaluated by in-situ tensile tests at 70 and 140 bar of hydrogen pressure. Tensile properties were studied in smooth and notched specimens ( $K_t=5.6$ ), following the ASTM G142 standard. The effect of hydrogen at the different working pressures is discussed in terms of the hydrogen embrittlement micromechanisms.

## 2. Steel and experimental procedure

### 2.1. Steel

The chemical composition of the 2205 DSS is given in Table 1. DSS plates were hot-rolled, then annealed at 1050°C and finally, quenched in water. DSS microstructure is illustrated in Fig. 1. The two phases, austenite (lighter) and ferrite (darker), are clearly identified in both orientations, leading to a banded microstructure.

Table 1. Chemical composition (wt. %)

Fe	C	Cr	Ni	Mo	Mn	Si
Balance	0.02	17	10	2	2	0.25

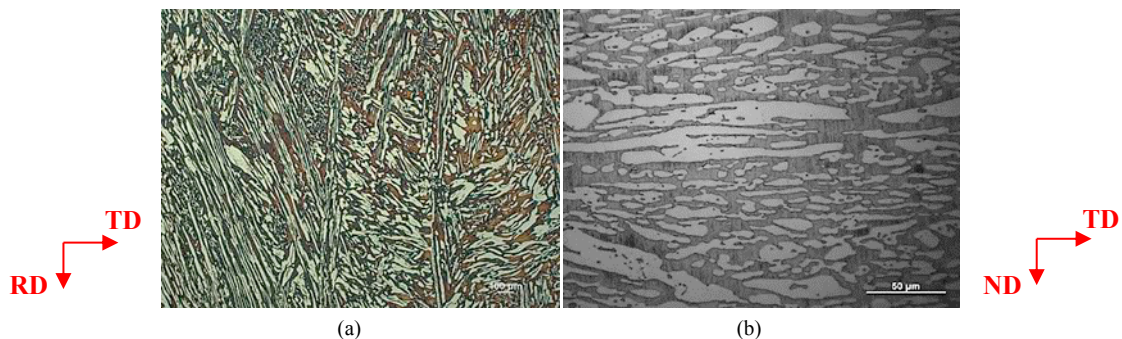


Fig. 1. 2205 DSS microstructures. (a) RD-TD orientation and (b) ND-TD orientation (thickness direction). Etching: electropolishing using 20g NaOH in 100 ml H<sub>2</sub>O with a voltage of 10V for 30s

### 2.2. In-situ tensile tests at high-pressure hydrogen gas

In-situ tensile tests were conducted following the ASTM G142 standard ‘Standard Test Method for Determination of Susceptibility of Metals to Embrittlement in Hydrogen Containing Environments at High Pressure,

High Temperature, or both.’ To evaluate hydrogen embrittlement sensitivity, smooth (Fig. 2a) and notched samples (Fig. 2b) were employed. Tensile load was applied parallel to the plate rolling direction (Fig. 2a,b,c).

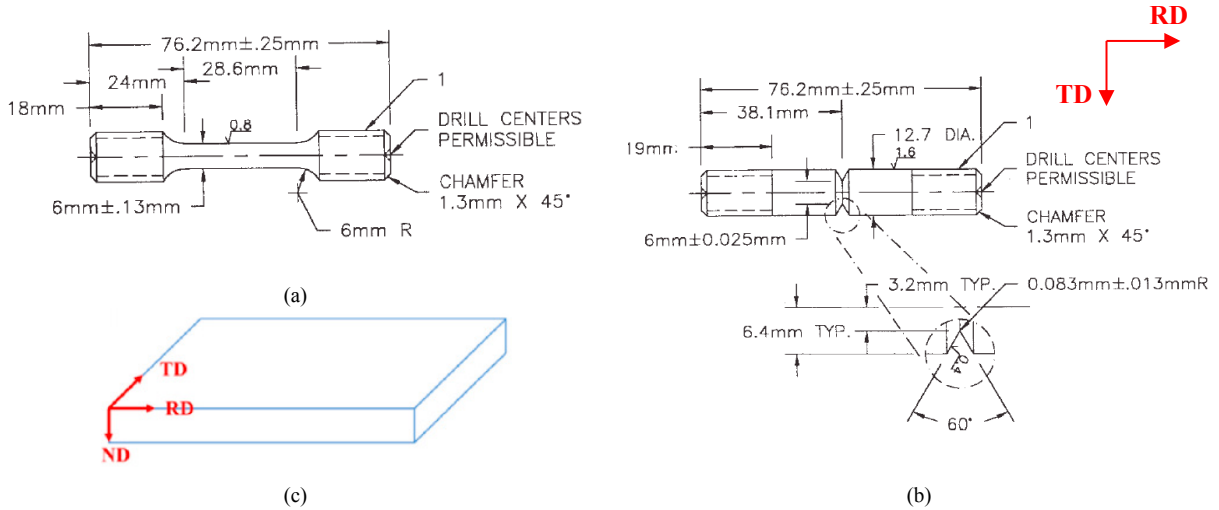


Fig. 2. Samples. (a) Smooth samples, (b) notched samples with  $K_t=5.6$  and (c) Plate orientation

First of all, tensile properties were determined in air (uncharged condition). Then, tensile tests were also obtained at 70 and 140 bar of hydrogen pressure. Tensile tests were carried out at 0.002 mm/s (0.12 mm/min) and room temperature (RT) in a high-pressure hydrogen facility (Fig. 3), available in the Hydrogen Technologies Research Laboratory at the University of Burgos (Spain). Hydrogen embrittlement was quantified by means of the hydrogen embrittlement index,  $EI$ , following equation (1).  $X$  and  $X_H$  represent the mechanical property evaluated in air (uncharged condition) and hydrogen gas atmosphere, respectively.  $EI$  can range from 0 (no embrittlement) to 100% (total loss of mechanical property).

$$EI = \frac{X - X_H}{X} \cdot 100 \tag{1}$$

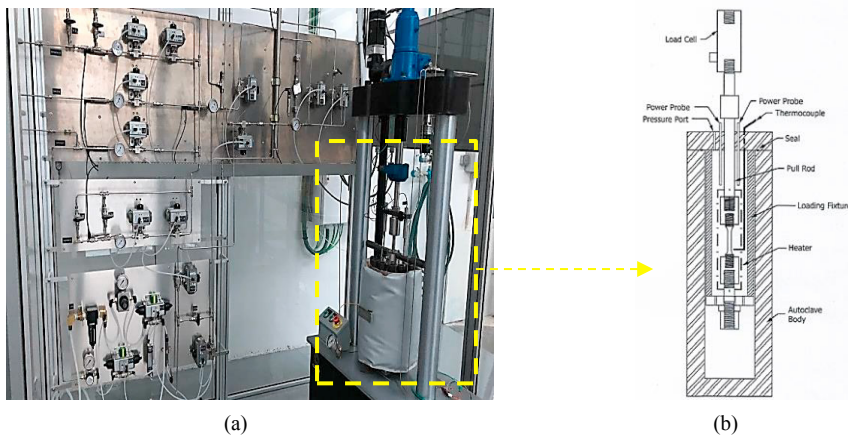


Fig. 3. (a) High-pressure hydrogen facility at the University of Burgos. (b) Schematic representation of a typical test cell designed to conduct HP/HT gaseous hydrogen embrittlement experiments (from ASTM G142 standard)

### 3. Results

Hydrogen high-pressure in-situ tensile results are given in this chapter. Besides, fracture micromechanisms are also discussed in terms of the hydrogen pressure.

#### 3.1. In-situ tensile tests in smooth samples and fracture surfaces

Tensile results obtained in air (uncharged condition) and hydrogen gas atmosphere (70 and 140 bar) are shown in Fig. 4, for a crosshead speed of 0.002 mm/s (0.12 mm/min). Based on the results displayed in Fig. 4, mechanical properties are summarized in Table 2, where  $\sigma_{YS}$  is the yield strength,  $\sigma_{UTS}$  represents the ultimate tensile strength,  $\epsilon$  is the elongation at fracture and RA is the reduction of area. The yield strength and the ultimate tensile strength were slightly affected by hydrogen. Nevertheless, the loss of ductility, in terms of elongation and reduction of area, was notably pronounced. Besides, the increase in hydrogen pressure from 70 to 140 bar seems to be negligible.

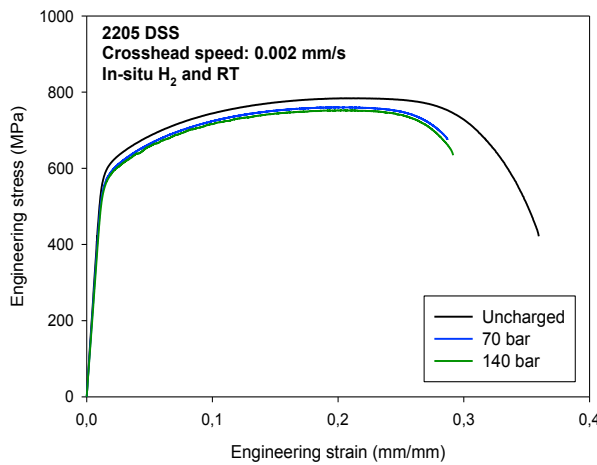


Fig. 4. Tensile curves. Smooth samples

Table 2. Mechanical properties. Smooth samples

	$\sigma_{ys}$ (MPa)	$\sigma_{UTS}$ (MPa)	$\epsilon$ (%)	RA (%)
Uncharged	574	784	36	89
70 bar	565	760	29	49
140 bar	560	752	29	48

Regarding the fracture micromechanisms, dimples indicating ductile fracture ( Fig. 5) were observed in air (uncharged condition). However, hydrogen assisted cracks were observed on the entire surface at 70 and 140 bar, as can be seen in Fig. 6. Austenite/ferrite interfaces decohesion were clearly noticed in Fig. 6(c). In further detail here, ferrite cleavage like fracture and austenite quasi-cleavage fracture with small breaches (white arrows) were also observed

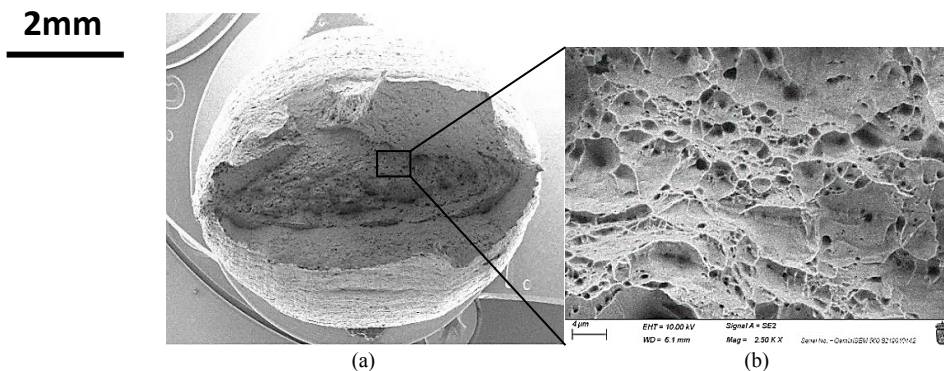


Fig. 5. Fracture micromechanism in air (uncharged). (a) General fracture surface. (b) Detail at 2500x with microvoids coalescence

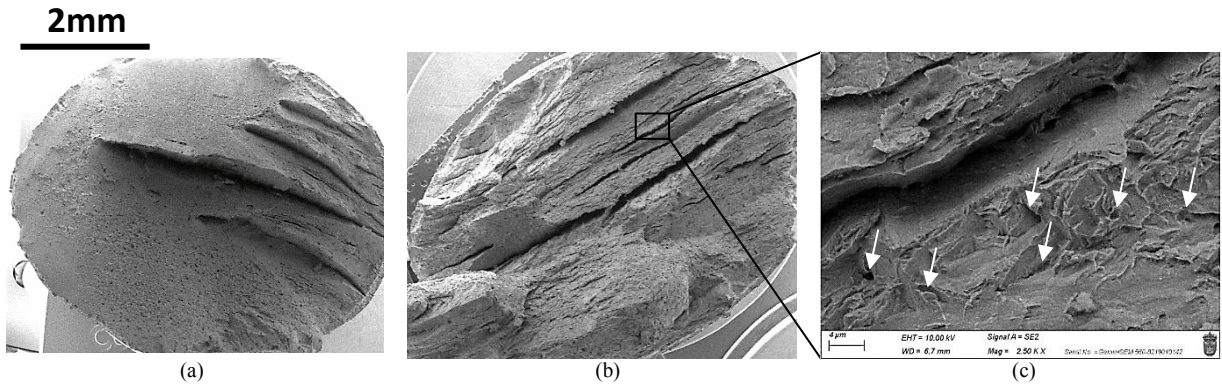


Fig. 6. Fracture micromechanims in hydrogen gas atmosphere. (a) General fracture surface at 70 bar. (b) General fracture surface at 140 bar. (c) Fracture detail (x2500) at 140 bar

3.2. In-situ tensile tests in notched samples and fracture surfaces

Hydrogen embrittlement susceptibility was also studied in notched samples. Tensile results, in air and hydrogen gas, are displayed in Fig. 7. The notch tensile strength (NTS) and reduction of area (RA) are introduced in Table 3. Unlike what has been observed in the smooth samples, hydrogen embrittlement improved when hydrogen pressure increased from 70 to 140 bar. At 140 bar, NTS decreased 34% (1360→896MPa) whilst, RA decreased 91% (34.3→3.2%).

Hydrogen clearly modified fracture micromechanims. For the uncharged samples, fracture surface showed clear dimples, indicating ductile fracture behaviour (Fig. 8a). However, for hydrogen in-situ tests at 70 bar, two different operative failure micromechanims were observed. In the outer zone, a brittle region (~200 μm depth) was observed, with secondary cracks growing internally (Fig. 8b). Nevertheless, dimples were also observed in the centre of the sample. On the other hand, for hydrogen in-situ tensile tests at 140 bar, hydrogen assisted cracks seem to nucleate directly from the notch tip surface. At higher magnification (2500x), flat cleavage facets in the ferrite and a rougher surface in the austenite were clearly observed (Fig. 8c).

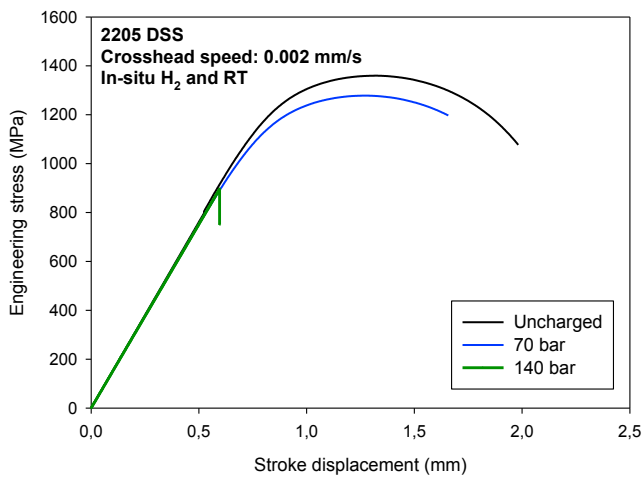


Fig. 7. Tensile curves. Notched samples (Kt=5.6)

Table 3. Mechanical properties. Notched samples (Kt = 5.6)

	NTS (MPa)	RA (%)
Uncharged	1360	34.3
70 bar	1278	15.3
140 bar	896	3.2

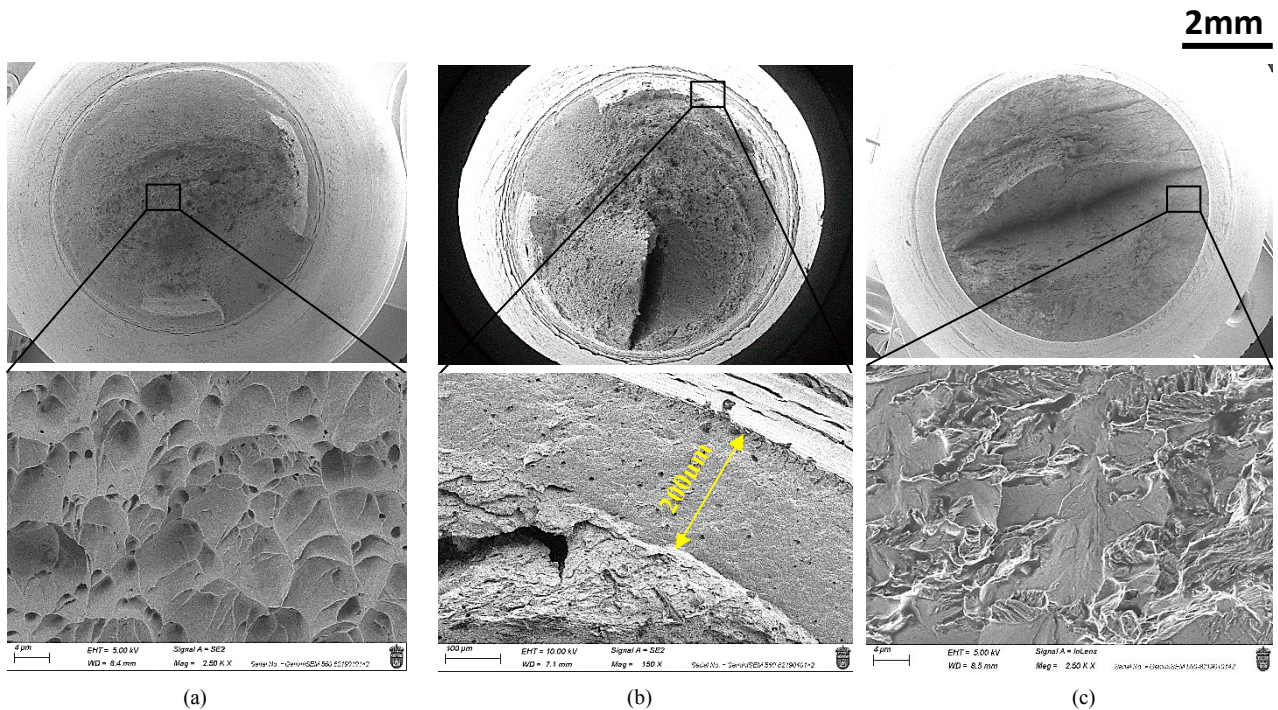


Fig. 8. Fracture micromechanisms. (a) In air (uncharged). (b) At 70 bar and (c) At 140 bar of hydrogen pressure

#### 4. Conclusions

In-situ tensile tests in high-pressure hydrogen gas were carried out in smooth and notched samples. The main conclusions are the following. In smooth samples, properties related with ductility, such as elongation and reduction of area, were especially affected. Hydrogen-assisted cracks were observed throughout the fracture surface. Despite of this fact, the increase in hydrogen pressure from 70 to 140 bar seems to be negligible. Regarding the notched samples, hydrogen embrittlement was notably improved with increasing hydrogen pressure. Hydrogen-enhanced decohesion micromechanisms were pronounced at 140 bar.

#### Acknowledgements

The authors would like to thank the Spanish Government for the financial support received to perform the research projects PID2021-124768OB-C21 and TED2021-130413B-I00–HyDuplex3D. This work was also supported by the Regional Government of Castilla y León (Junta de Castilla y León) and by the Ministry of Science and Innovation MICIN and the European Union Next Generation EU/PRTR (MR4W.P2 and MR5W.P3).

#### References

- [1] Arniella V, Álvarez G, Belzunce J, Rodríguez C. Hydrogen embrittlement of 2205 duplex stainless steel in in-situ tensile tests. *Theoretical and Applied Fracture Mechanics* 2023;124. <https://doi.org/10.1016/j.tafmec.2023.103794>.
- [2] Claeys L, De Graeve I, Depover T, Verbeke K. Hydrogen-assisted cracking in 2205 duplex stainless steel: Initiation, propagation and interaction with deformation-induced martensite. *Materials Science and Engineering: A* 2020;797. <https://doi.org/10.1016/j.msea.2020.140079>.
- [3] Wu W, Liu S, Li W, Li J. Identification of microstructure factors affecting hydrogen embrittlement of a 2205 duplex stainless steel. *Corros Sci* 2022;208. <https://doi.org/10.1016/j.corsci.2022.110643>.